HOKKAIDO UNIVERSITY

Title	Precursory tilt changes of small phreatic eruptions of Meakan-dake volcano, Hokkaido, Japan, in November 2008
Author(s)	Aoyama, Hiroshi; Oshima, Hiromitsu
Citation	Earth planets and space, 67, 119 https://doi.org/10.1186/s40623-015-0289-9
Issue Date	2015-07-29
Doc URL	https://hdl.handle.net/2115/59830
Rights(URL)	https://creativecommons.org/licenses/by/4.0/
Type	journal article
File Information	EPS_67_119.pdf

Hokkaido University Collection of Scholarly and Academic Papers : HUSCAP

Aoyama and Oshima *Earth, Planets and Space* (2015) 67:119
DOI 10.1186/s40623-015-0289-9

Earth, Planets and Space
a SpringerOpen Journal

FULL PAPER Open Access

Precursory tilt changes of small phreatic eruptions of Meakan-dake volcano, Hokkaido, Japan, in November 2008

Hiroshi Aoyama[1*] and Hiromitsu Oshima[2]

Abstract

Although forecasting an occurrence of phreatic eruption is very difficult, it has been reported that some precursory activities often precede these eruptions at several volcanoes. In this study, we observed seismic activities before and during the 2008 phreatic eruption at Meakan-dake volcano, eastern Hokkaido, Japan, by using broadband seismometers and surface mount-type tiltmeters. The precursory increase in seismicity began in late September about 2 months before the first eruption on November 18. After several rises and falls in seismicity in October and in early November, a small volcanic tremor was observed early on November 16. Although the original velocity seismogram of the tremor generally appeared to be spindle shaped, an outstanding ramp function appeared in the displacement seismogram obtained by simple integration. Since the ramp function appeared only in the horizontal components and continued for about 3 min, which is sufficiently longer than the natural period of the seismometer, we regarded the ramp function as an expression of the tilting motions of seismic stations that was quantitatively confirmed by the strong similarity between horizontal displacement seismograms and tilt data from co-located biaxial tiltmeter. Azimuthal distribution of three tilting vectors obtained from broadband seismograms was not consistent with a simple spherical source but rather strongly suggested a vertical dike under the crater. In this study, we confirmed that an almost vertical single dike effectively explains the observed tilting vectors. The estimated volume increase in the dike was 4–5 × 10^4 m^3. The strike direction of the dike is highly consistent with the alignment of the hydrothermal area on and around the volcano. Our dike model also partially explains the changes in global navigation satellite system (GNSS) measurement and in groundwater levels reported in previous research. Since a similar deformation coincided with a volcanic tremor preceding the 2006 eruption, we interpret that this must be an important preparatory process of phreatic eruptions at Meakan-dake volcano.

Keywords: Phreatic eruption; Precursory activity; Hydrothermal system; Ground deformation; Volcanic tremor; Broadband seismometer; Tilt response; Meakan-dake volcano

Background

Meakan-dake volcano (1499 m), situated on the western edge of Akan caldera, is an active volcano in Hokkaido. Since the first recorded eruption in 1955, this volcano has emitted small eruptions repeatedly from the summit craters (e.g., Sakuma and Murase 1957; Yokoyama et al. 1976; Kasahara 1988). All of the eruptive activities observed at Meakan-dake during the historical age were phreatic eruptions (Yokoyama et al. 1976; Ishimaru et al. 2009).

Phreatic eruption is defined as an explosion of a confined pocket of steam and gas with no direct involvement of fresh magma (e.g., Barberi et al. 1992). It occasionally appears as a prologue of magmatic eruptions (e.g., Matsumoto et al. 2013; Nakamichi et al. 2013) and also occurs without any associated magmatic eruptions such as those of Meakan-dake. The basic process of phreatic eruption is believed to be concerned with a rapid state change in the shallow hydrothermal system triggered by an increase in heat supply to underground water or a decrease in confining pressure of a

* Correspondence: aoyama@uvo.sci.hokudai.ac.jp
[1]Institute of Seismology and Volcanology, Faculty of Science, Hokkaido University, N10W8, Kita-ku, Sapporo, Hokkaido 060-0810, Japan
Full list of author information is available at the end of the article

© 2015 Aoyama and Oshima. This is an Open Access article distributed under the terms of the Creative Commons Attribution License (http://creativecommons.org/licenses/by/4.0), which permits unrestricted use, distribution, and reproduction in any medium, provided the original work is properly credited.

shallow superheated aquifer (e.g., Barberi et al. 1992; Germanovich and Lowell 1995). Several mechanisms for phreatic eruption have been proposed on the basis of field survey and theoretical consideration (e.g., Feuillard et al. 1983; Mastin 1991; Germanovich and Lowell 1995). However, the physical processes of phreatic eruption are still not fully understood.

Although phreatic eruption does not blow out juvenile magma, it is a highly explosive phenomenon and thus wreaks severe damages to the adjacent areas of the crater by strong blasts, volcanic bombs, and heavy ash falls. To reduce the risks of volcanic disaster, in addition to gaining a better understanding of the physical processes of phreatic eruption, elucidation of the preparatory processes of eruption is required. Barberi et al. (1992) compiled the precursory activities of phreatic eruptions reported in scientific papers and found that almost two thirds of the compiled events accompanied some sort of precursory variation in seismicity and in the chemical components of underground water. Although they concluded that phreatic eruptions have precursory phenomena, they also indicated the difficulties in singling out specific precursors of eruptions based on the available data. Even if an adequate number of instruments for physical monitoring were used on and around the intended volcano, it would be generally difficult to evaluate future activities from the observed data up to a given time. Therefore, acquiring a sufficient number of experiences at many volcanoes is indispensable for extracting the common features of phreatic eruption to effectively understand its preparatory processes.

Despite their minuscule magnitudes of eruption, seismic swarms and volcanic tremors often preceded the phreatic eruptions at Meakan-dake volcano (Japan Meteorological Agency 2013). The 2006 eruption was the first event recorded in the monitoring of a sequence of seismic activity toward the eruption at Meakan-dake by using a broadband seismometer. Aoyama and Oshima (2008) reported that an unusual, very long-period horizontal displacement was superimposed on the volcanic tremor that occurred almost 1 month before the eruption. They interpreted this activity as a tilt motion excited by the deflation of an isotropic source assumed to exist below the summit crater. Preceding the last eruption in November 2008, several seismic activities were observed as precursory phenomena. Similar to the 2006 activity, we found a very long-period signal superimposed on the volcanic tremor, which occurred 2 days before the eruption. In this study, we analyze the precursory long-period signal that preceded the 2008 eruption to gain greater understanding of the preparatory process of the phreatic explosions at Meakan-dake volcano. Since the data available for our analysis are quite limited because of a small number of observations, our objective here is to give a realistic and conceivable image of the precursory activity of the phreatic explosion rather than to precisely estimate the geometrical configuration of the source that excited the long-period signal.

Methods

Recent activities and the 2008 eruption of Meakan-dake volcano

Meakan-dake volcano is a volcanic complex of eight small volcanoes that erupted from independent conduits (Wada 1991). Major volcanic edifices include Naka-Machineshiri, Pon-Machineshiri, and Akan-fuji, and fumarolic activity is evident in the craters of Naka-Machineshiri and Pon-Machineshiri (Fig. 1). Naka-Machineshiri is the biggest and oldest edifice and consists mainly of dacitic and andesitic lava and lava domes. Formation of the Pon-Machineshiri edifice began around 7 ka on the southern flank of Naka-Machineshiri. Akan-fuji is the youngest edifice and emitted repeated magmatic eruptions between 2.5 and 1 ka. After the activity of Akan-fuji, repeated phreatic eruptions and pyroclastic activity produced the present summit craters of Pon-Machineshiri and Naka-Machineshiri (Wada 1998).

The first recorded eruption at Meakan-dake volcano occurred at the southern rim of the summit crater of Pon-Machineshiri on November 19, 1955 (e.g., Sakuma and Murase 1957; Murase 1957). Since then, small phreatic eruptions had been repeated at Pon-Machineshiri and Naka-Machineshiri until 1966 (Yokoyama et al. 1976). Early geophysical works successfully noted preceding increases in seismic activity prior to phreatic eruptions in 1956 and 1959 (e.g., Sakuma and Murase 1957; Murase et al. 1960). After a dormant period of about 22 years, small phreatic eruptions occurred again in 1988 in the craters produced by the 1955 eruption (Kasahara 1988). Then, the volcano experienced five active periods of small phreatic eruptions in 1988, 1996, 1998, 2006, and 2008. Except for the 1998 activity, seismic swarms or volcanic tremors preceded the eruptive activities by a few months (Fig. 2). Therefore, temporal fluctuation in seismic activity has been a good indicator of volcanic unrest at Meakan-dake volcano.

Precursory activity of the 2008 eruption, the first seismic swarm, began in the evening of September 26 almost 52 days before the eruption. In the afternoon of September 29, a volcanic tremor 4 min in duration occurred, followed by an abrupt increase in the frequency of occurrence of volcanic earthquakes. The first swarm continued for almost 4 days until September 30. After a small increase in seismicity on October 12, the second seismic swarm emerged from October 19 to 28. The seismicity of the second swarm was weaker than that of the first swarm, and volcanic tremors were not observed during this period. The third seismic swarm was then observed from November 9 to 12. The daily rate of

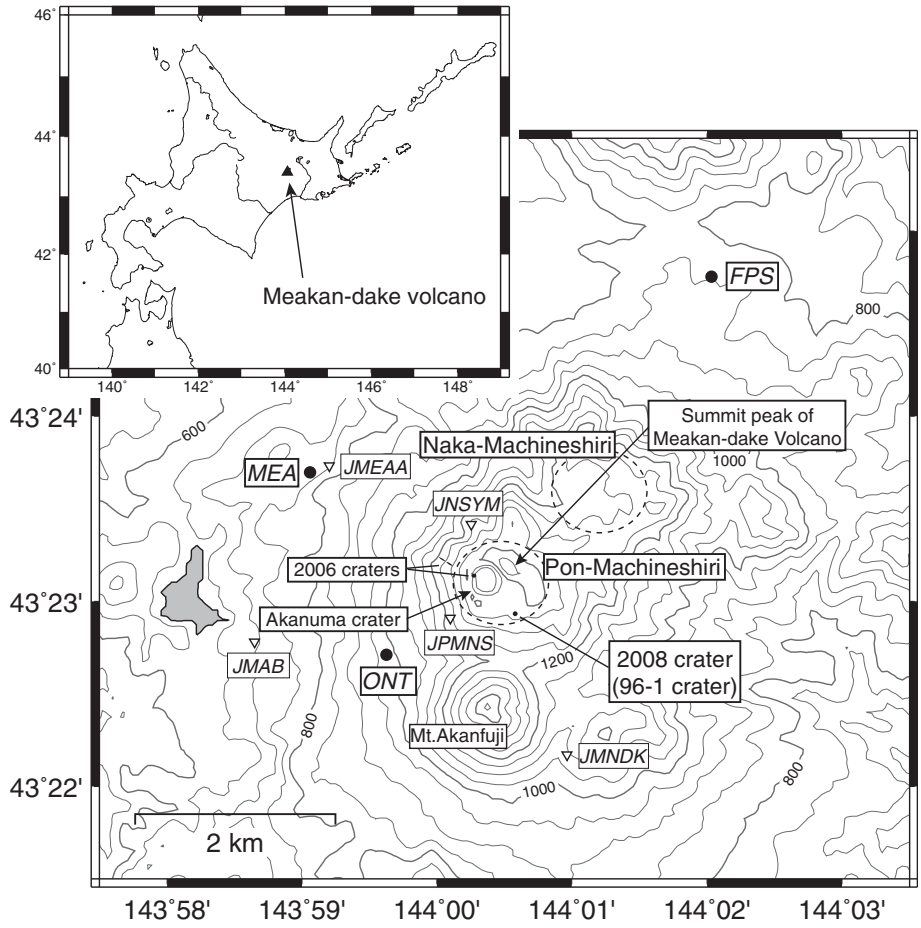

Fig. 1 Contour map and station distribution around Meakan-dake volcano. *Black circles* indicate broadband seismic stations from which the data used in this study was obtained. *Outlined inverted triangles* express seismic stations with short-period seismometers operated by Sapporo District Meteorological Observatory, Japan Meteorological Agency. *Dotted circles* show summit crater areas of Naka-Machineshiri and Pon-Machineshiri. There are several craters within the Pon-Machineshiri crater. The 2008 eruption occurred at the 96-1 crater on the southern rim of the Pon-Machineshiri crater. The 2006 eruption opened new pits in the northwestern rim of the Akanuma crater, on the opposite side of the Pon-Machineshiri crater

volcanic earthquakes increased to more than 200 on November 11. After a temporary lull in seismicity, a second remarkable volcanic tremor occurred at 00:56 JST on November 16. This tremor continued for about 30 min but was smaller in amplitude than the first one occurring on September 29. Subsequently, volcanic tremors of long duration were intermittently observed from November 17 to 19. During the daytime on November 18, a volcano monitoring video camera at Sapporo District Meteorological Observatory, Japan Meteorological Agency, hereafter referred to as JMA Sapporo, detected through wisps of clouds substantial ash covering the snow surface on the southern slope of Pon-Machineshiri. Although no seismic or infrasonic signal indicated the occurrence of an explosion, it was concluded that the first phreatic eruption occurred before dawn on November 18, based on visual observation, weather conditions, and tremor activity. About 10 days later, a phreatic eruption occurred again on November 28. The total amount of volcanic ejecta discharged during the 2008 eruptive activity was estimated by field survey to be about 12,000 tons (Ishimaru et al. 2009), which is almost the same as that of the 2006 eruption at 9000 tons (Hirose et al. 2007a), almost one third that of the 1996 eruption at 36,000 tons (Hirose et al. 2007b), and almost 11 times that of the 1998 eruption at 1100 tons (Hirose et al. 2007b).

A preliminary report on the 2008 eruption by Ishimaru et al. (2009) indicated that the volcanic ash consisted mainly of rounded particles of andesitic rock. Since no fragments of pumice from juvenile magma were present, they concluded that the ash deposits exhibited features of phreatic eruption. They also reported a small step-like extension of a few millimeters in the relative location between the global navigation satellite system (GNSS) receivers installed across the Pon-Machineshiri crater.

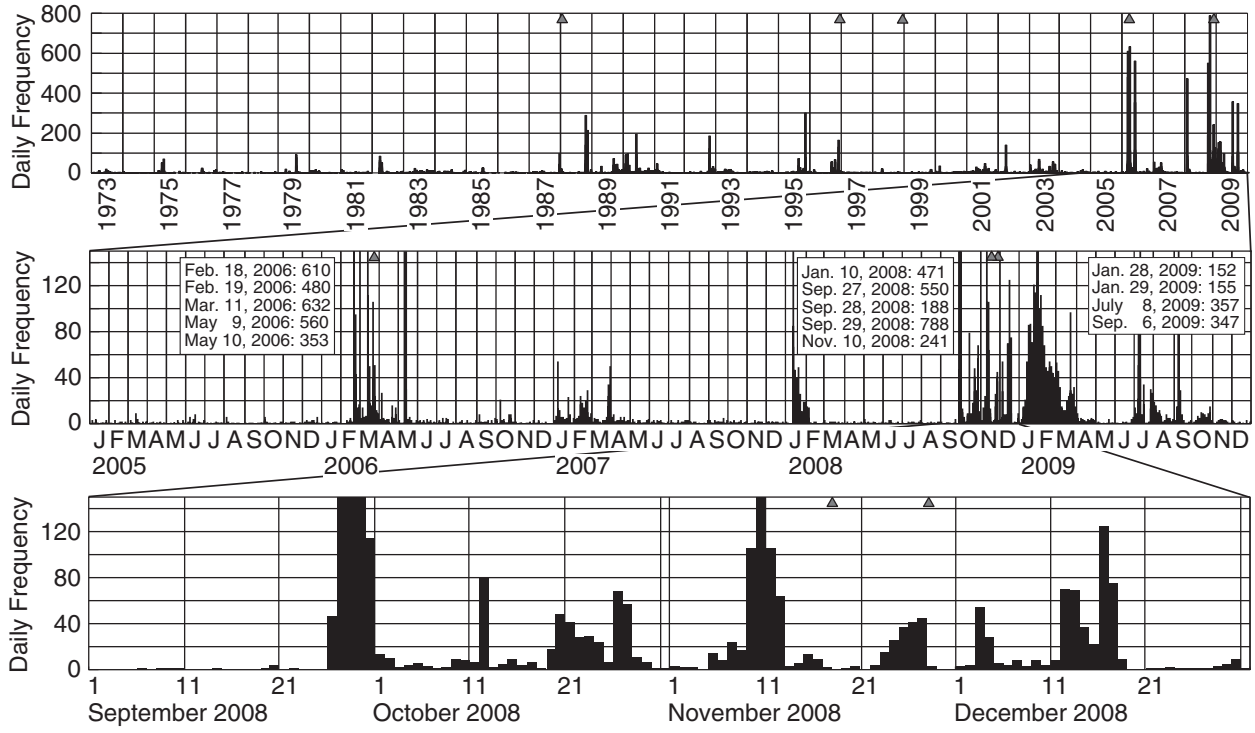

Fig. 2 Daily frequency of volcanic earthquakes at Meakan-dake volcano. The *top graph* shows long-term seismicity since 1973 recorded by Sapporo Meteorological Observatory, Japan Meteorological Agency. Five recent eruptions are included in this period. The middle graph expresses medium-term seismicity since 2005, which includes the eruptions in 2006 and 2008. The bottom graph shows short-term seismicity during 4 months from September to December 2008. *Gray triangles* at the top of each graph express eruptive activities. No evident increase in seismicity was observed prior to the eruption in 1998. However, intense seismic activities with no subsequent eruption have been observed

Although this change was not associated with the eruptions of November 18 and 28, it was observed on November 16, the same day that the second remarkable volcanic tremor occurred. Coinciding with the tremor, a step-like increase in groundwater level was also observed at their observational well in Akanko Onsen, which is about 8 km northeast (NE) of Meakan-dake. These observations by Ishimaru et al. (2009) strongly suggest ground deformation coincident with the tremor on November 16.

Seismic observation and data

Meakan-dake volcano has been designated as an active volcano to be monitored continuously by the Coordinating Committee for the Prediction of Volcanic Eruptions. JMA Sapporo began seismic monitoring at the northwest (NW) foot of Meakan-dake volcano in 1973. The number of seismic stations operated by JMA Sapporo has been increased in phases since 2000, and hypocenter determination of volcanic earthquakes began as routine analysis in 2004. Although JMA Sapporo increased the number of stations, instruments installed at the JMA stations are mainly short-period seismometers and low-frequency microphones; therefore, its monitoring network lacks the ability to observe slow phenomena of longer than a few seconds. To detect long-period events, the Institute of Seismology and Volcanology, Hokkaido University, hereafter referred to as ISV, operates a broadband seismometer at Meakan Onsen, hereafter referred to as MEA, which is about 2.0 km NW of Pon-Machineshiri. In response to the phreatic eruption in March 2006 (Aoyama and Oshima 2008), ISV added two broadband seismic stations during the summer season in 2006 (Fig. 1). To improve the azimuthal coverage, new stations, stations ONT and FPS, were installed at the southwest (SW) flank of Pon-Machineshiri and at NE flank of Naka-Machineshiri, respectively. During the active period in 2008, Güralp CMG-40T broadband seismometers (flat velocity response, 0.033–50 Hz) were operated at all three stations. The sensor outputs were digitized by a Hakusan LT8500 data converter with 22-bit precision at a sampling rate of 200 Hz at MEA in addition to a Hakusan LS7000XT data converter with 24-bit precision at sampling rates of 100 Hz at ONT and 200 Hz at FPS. These outputs were then transmitted to ISV through radio transmission and telephone lines. A surface mount-type biaxial tiltmeter, Applied Geomechanics T701-2A, was also installed at MEA and FPS together with CMG-40T, which enabled us to

examine the tilt effects on seismograms. Outputs from the tiltmeter were digitized with 18-bit precision at a sampling rate of 1 Hz at MEA and with 24-bit precision at a sampling rate of 200 Hz at FPS.

As previously mentioned, two remarkable volcanic tremors occurred before the first eruption on November 18: the first at 14:11 JST on September 29 and the second at 00:56 JST on November 16. The maximum amplitude of ground displacement recorded by a short-period seismometer at station JMAB which is operated by JMA Sapporo was 2.4 μm for the first tremor and 0.5 μm for the second. Both events were successfully observed by the broadband seismometers and tiltmeters installed at the three stations. We investigated the seismic and tilt data to determine the existence of long-period signals that may suggest ground tilt motion at the station by following the same procedure as that reported by Aoyama and Oshima (2008). Despite the large amplitude of seismic tremor, we were unable to detect a notable long-period signal exceeding the background noise level in the broadband seismic traces of the first tremor. However, it was confirmed that the small second tremor occurring on November 16 contained an unusual long-period signal, particularly in the horizontal components. This long-period signal appeared almost coincidentally at all three stations. Figure 3 shows the waveforms recorded at MEA and ONT by the CMG-40T seismometer and the T701-2A biaxial bubble tiltmeter (MEA only). It is clear that a volcanic tremor began around 00:56 JST in all components of the velocity traces. However, it was quite difficult to recognize the tremor signal in the displacement traces obtained by simple integration after removal of the direct current (DC) component from the velocity traces. Instead, long-period signals such as that of the ramp function appeared in the east–west (EW) component of displacement traces at ONT. We detected similar fluctuation in the EW component of displacement and tilt traces at MEA at almost the same time. It should be noted that the displacement seismogram of CMG-40T and the tilt waveform obtained by T701-2A are quite similar. As is shown subsequently, the horizontal displacement of a seismometer is proportional to the tilt angle in a frequency range lower than the natural frequency of the seismometer. Since the duration of this signal was about 3 min, which is significantly longer than the natural period of CMG-40T at 30 s, the change in horizontal displacement does not express the pure translational motion but rather reflects the ground tilt.

Estimation of tilt motion from seismogram data

When the ground at a monitoring station inclines, the tiltmeter and the horizontal components of the seismometer are affected by the change in gravitational acceleration. Following the formulation given by Graizer (2006), Aoyama (2008) presented a quantitative relationship between the velocity response function and the tilt response function of a CMG-40T seismometer and confirmed its validity by conducting a laboratory experiment. The relation can be expressed as

$$C_T(\omega) = \frac{g}{-\omega^2} C_v(\omega) \tag{1}$$

where $C_T(\omega)$ is the tilt step response function, $C_v(\omega)$ is the velocity impulse response function, g is the gravitational acceleration, and ω is the angular frequency of the input signal. $C_v(\omega)$ for the CMG-40T seismometer can be calculated by using the distribution of poles and zeros, p_i and z_i (i = 1–3) as

$$C_v(\omega) = -0.314 \frac{(i\omega - z_1)(i\omega - z_2)(i\omega - z_3)}{(i\omega - p_1)(i\omega - p_2)(i\omega - p_3)} \tag{2}$$

Substituting the pole and zero values given by the manufacturer in this equation (e.g., Table 2 of Aoyama and Oshima 2008) and taking the low-frequency limit, we can obtain a theoretical conversion value of 0.223 mm/μrad (=4.48 μrad/mm). Using this value, the apparent displacement of the seismogram due to tilting motion can be transferred to the angle of tilt change in the frequency range of $\omega << \omega_0$, where ω_0 is the natural angular frequency of the seismometer. The same relationship between the seismometer displacement and tilt change was also reported by Genco and Ripepe (2010), in which this relationship was applied to extract the tilt motion due to precursory inflation of a Strombolian eruption from the CMG-40T seismogram. Takeo et al. (2013) also applied this method to obtain tilt motion prior to Vulcanian eruptions at Shinmoe-dake volcano in 2011.

Particle orbits projected on the horizontal plane during the gray-shaded period in Fig. 3 are shown in Fig. 4. Tilting vectors can be obtained from these particle orbits by using the conversion value given above. The direction of apparent horizontal displacement corresponds to the uplift direction; hence, the eastward displacement observed at ONT represents an uplift of the eastern side of the station. The direction of uplift and amplitude of tilt change at the three seismic stations are estimated by connecting a straight line between start and end points of each particle orbit in Fig. 4 as N288° E/0.14 μrad at MEA, N83° E/0.48 μrad at ONT, and N222° E/0.13 μrad at FPS. Although the orbits at MEA and FPS have some minor deviations from a straight line, and variations of tilt direction within a few degrees are conceivable, the comprehensive tilt motions are well represented by the linear tilt vectors shown in Fig. 4. Arrows in the map view in Fig. 5 express the spatial distribution of the tilt change.

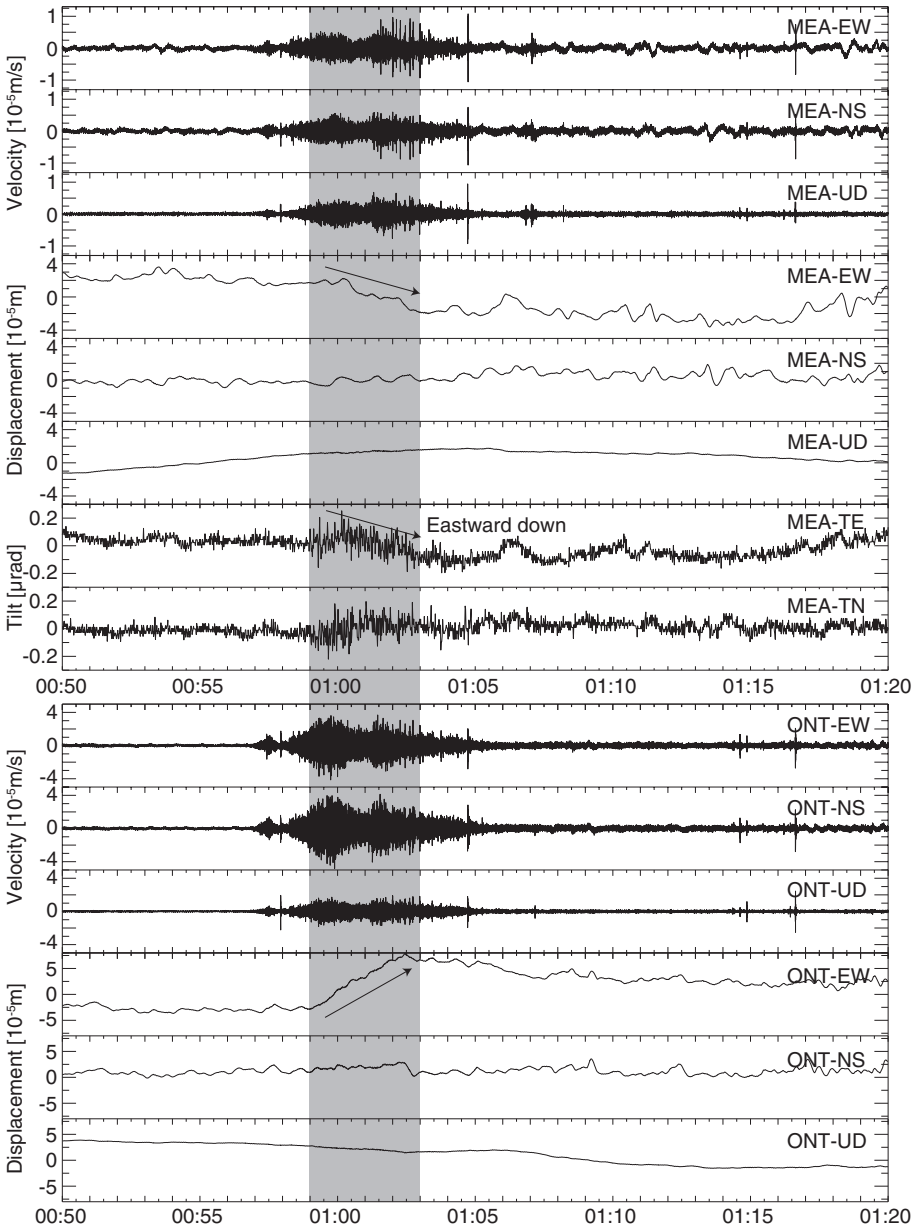

Fig. 3 Waveforms of the volcanic tremor on November 16, 2008. *Top panel* shows seismic and tilting data obtained by a broadband seismometer and tiltmeter at station MEA. For seismic data, displacement waveforms obtained by a simple integration of the original velocity seismogram are also displayed. The *bottom panel* shows the seismogram operated at ONT. The horizontal axis expresses local time in Japan on November 16. A spindle-shaped signal of volcanic tremor in the velocity waveforms at around 1:00 is evident. However, a clear ramp function appears in the horizontal components of the displacement waveforms. During the period, indicated by *gray shading*, large apparent eastward displacement was observed at ONT. At the same time, relatively small but discernible displacement was also recorded at MEA. It should be noted that the horizontal displacement waveforms closely resemble tilting waveforms recorded by a tiltmeter

Estimation of deformation source

Spatial distribution of tilt motions implies a clue to the geometric configuration of a deformation source. Two stations, ONT on the SW flank and FPS on the NE flank, indicate uplift of the summit area, whereas MEA on the NW flank shows subsidence of the summit direction. Such variation of the observed tilt motions may be explained by a non-isotropic source having azimuthal dependence on the surface deformation. Here, because we have only three tilt vectors, a single deformation source with simple configuration should be considered. Simple volumetric sources commonly assumed in the analysis of volcano deformation include spheres, pipes, dikes, and sills (e.g., Lisowski 2007). Although non-

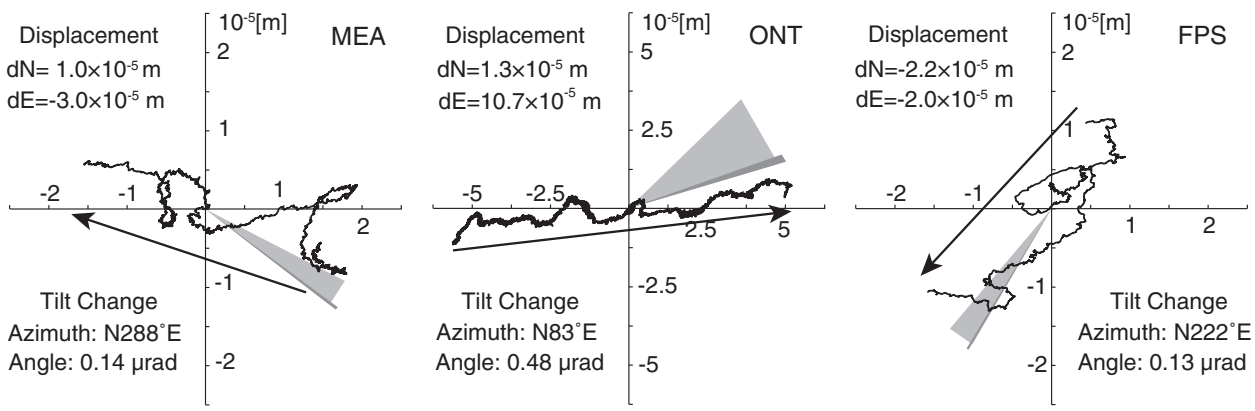

Fig. 4 Displacement particle orbits during the *gray-shaded period* in Fig. 3. An *arrow* placed in each graph expresses the direction of trajectory. *Dark-* and *light gray-colored triangles* in each graph indicate azimuth directions of the 96-1 crater and that of the Pon-Machineshiri crater area from each station, respectively. It should be noted that a different scale is used for ONT

volumetric faulting can generate crustal deformation, it is unlikely to continue fault motion up to a few minutes at a shallow depth of a volcano. Among these candidates of simple deformation source, spherical and vertical pipe sources were excluded because these sources produce only axisymmetric surface deformation. Although an inclined pipe source and sill-like source can generate non-axisymmetric deformation, it is difficult to reproduce the reversal polarity of tilting motion at MEA. However, an expanding vertical dike striking in the NW–southeast (SE) direction located under the Pon-Machineshiri crater could explain a spatial pattern of the observed tilt changes including the reverse polarity at MEA. Therefore, we assumed a dike below the crater as the single

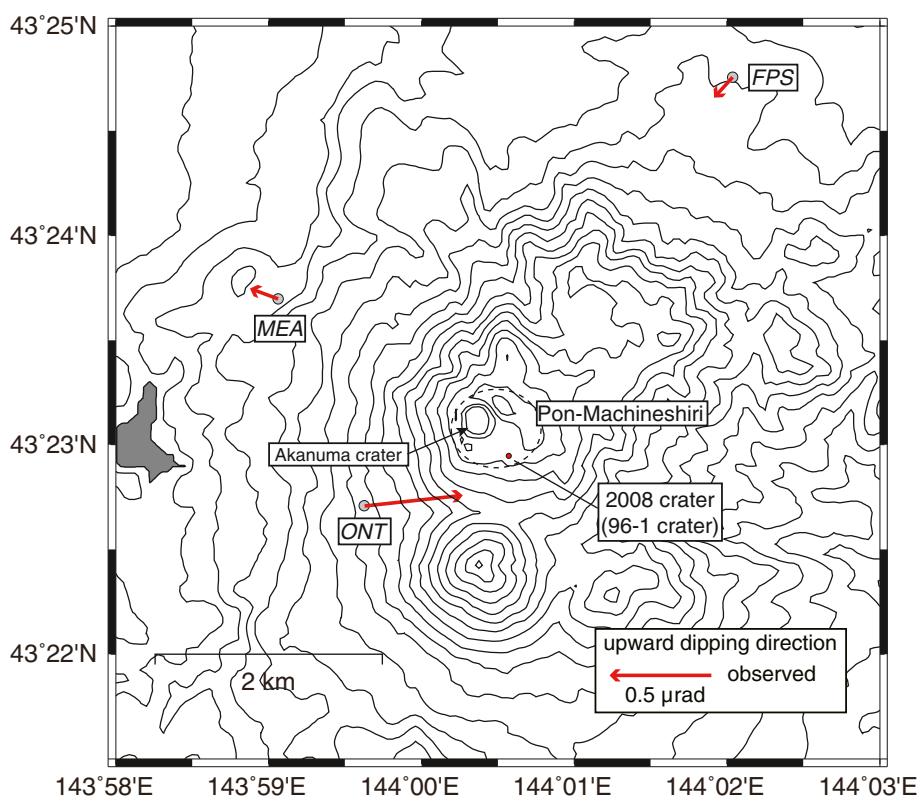

Fig. 5 Map view of the observed tilting vectors. Upward dipping directions are shown by arrows. Although the vectors at ONT and FPS almost point to the Pon-Machineshiri crater area, subsidence of crater direction was observed at MEA

deformation source and estimated its depth, strike, dip, length, width, and opening by using the grid search approach.

The theoretical tilting motion was calculated by the analytical expression given in Okada (1992). Since a shallow source is expected, station elevation was considered in the calculation by varying the source depth relative to each station (Williams and Wadge 1998). To treat small tilt changes at MEA and FPS in the same manner as the large change at ONT, the fitness of calculated and observed tilt vectors was evaluated by using the squared sum of normalized residuals:

$$E = \sum_{i=1}^{3}\left(\frac{(\mathrm{OT}x_i - \mathrm{ST}x_i)^2}{\mathrm{OT}x_i^2} + \frac{(\mathrm{OT}y_i - \mathrm{ST}y_i)^2}{\mathrm{OT}y_i^2}\right) \quad (3)$$

where $\mathrm{OT}x_i$ and $\mathrm{OT}y_i$ are the observed tilt changes in x and y directions at the i-th station, respectively, and $\mathrm{ST}x_i$ and $\mathrm{ST}y_i$ are the calculated tilt changes in x and y directions at the i-th station, respectively.

The centroid of the rectangular dike was assumed to be located just below the 96-1 crater (E144.0090°, N43.3825°) on the SE edge of the Pon-Machineshiri crater from which volcanic materials were ejected in the 2008 eruption (Ishimaru et al. 2009). To find the best-fit parameters, we divided the search into three steps including a rough search in wide parameter ranges and two finer searches in narrow ranges. In the first rough estimation, we assumed a purely vertical dike and changed the dike parameters in the range of 0.1–1.9 km below sea level (bsl) for the dike centroid depth D (0.2 km step), N110° E–N130° E for the strike direction Φ (2° step), 0.2–4.2 km for the dike length L in the strike direction (0.4 km step), 0.2–1.4 km for the dike width W in the dip direction (0.2 km step), and 1.0–5.0 cm for the dike opening U (1.0 cm step). The second fine search was performed around the best solution of the first step with the changing dip angle δ. Parameter ranges include $D = 0.1$–0.5 km bsl (0.02 km step), $\phi =$ N110° E–N125° E (1° step), $\delta = 70°$–$90°$ (2° step), $L =$ 0.2–4.0 km (0.2 km step), $W = 0.2$–1.4 km (0.2 km step), and $U = 1.0$–5.0 cm (1 cm step). In the third step, we found the final fitting solution by changing the parameters around the solution of the second step as D every 0.01 km in 0.26–0.29 km bsl, ϕ and δ every 1° in 80°–90° and 120°–126°, L and W every 0.1 km in 0.2–4.0 km and 0.2–1.6 km, and U every 0.1 cm in 0.4–3.0 cm.

Results and discussion

We obtained the best-fit solution at $D = 0.27$ km bsl, $\phi =$ N122°E, $\delta = 84°$, $L = 3.2$ km, $W = 1.2$ km, and $U = 1.3$ cm. Figure 6a shows observed and calculated tilt vectors of the final fitting in the map view (case 1). A single dike below the 96-1 crater well reproduced the observed tilt directions and amplitudes at the three stations around the volcano. The volumetric change due to the dike opening became about $\Delta V = 5.0 \times 10^4$ m^3.

To examine the effect of horizontal location of the dike centroid on the estimated parameters, we performed an additional search in the same manner by assuming a dike below Akanuma crater (E144.0064°, N43.3856°), which is the largest crater in Pon-Machineshiri. New pits opened at the NW perimeter of this crater during the 2006 eruption (Aoyama and Oshima 2008). In this case, the best-fit solution was obtained as a combination of parameters of $D = 0.26$ km bsl, $\phi =$ N119°E, $\delta = 87°$, $L = 2.3$ km, $W = 0.6$ km, and $U = 2.8$ cm. A comparison of the observed and calculated tilt vectors is shown in Fig. 6b (case 2). In both cases of fitting, an almost vertical dike directed toward MEA was estimated to reproduce subsidence in the summit direction at MEA. The length of the dike became shorter in the second case because the assumed location of dike centroid is closer to MEA than that in the first case. However, the volumetric change of the dike in the second case was about $\Delta V = 3.9 \times 10^4$ m^3, which is almost the same as that in the first case.

According to these parameter searches, we quantitatively confirmed that a single dike below the Pon-Machineshiri crater effectively explains the tilt motion observed during the volcanic tremor on November 16. Since we have only three tilt datasets for this event, we did not pursue a better solution for minimizing the residual by making the searching grid step finer.

Meakan-dake volcano experienced a phreatic eruption of similar size in March 2006. Almost 1 month prior to the eruption on March 21 of that year, the first precursory seismic swarm began (Aoyama and Oshima 2008). During the swarm period, two volcanic tremors were identified, one of which was accompanied by a long-period signal in the horizontal component of the broadband seismogram at MEA. The seismometer CMG-40T at MEA was continuously operated without relocation and replacement from 2006 to 2008. Thus, we can directly compare the tilt signal overlapped with the volcanic tremors.

The downward dipping vector at MEA for the 2006 event was approximately toward the summit crater area, as was the case for the 2008 event. The tilt amplitude was calculated as 0.94 μrad from the apparent displacement offset of 0.21 mm (Aoyama and Oshima 2008), which is about 6.7 times larger than that of the tilt in the 2008 event at ~0.142 μrad at MEA. The signal duration of the tilting motion in the 2006 event was about 1 min, whereas it was about 3 min in the 2008 event. Since MEA was the only broadband seismic station operated in 2006, the tilt change in the 2006 event was explained by deflation of the spherical source located beneath the Pon-Machineshiri crater (Aoyama

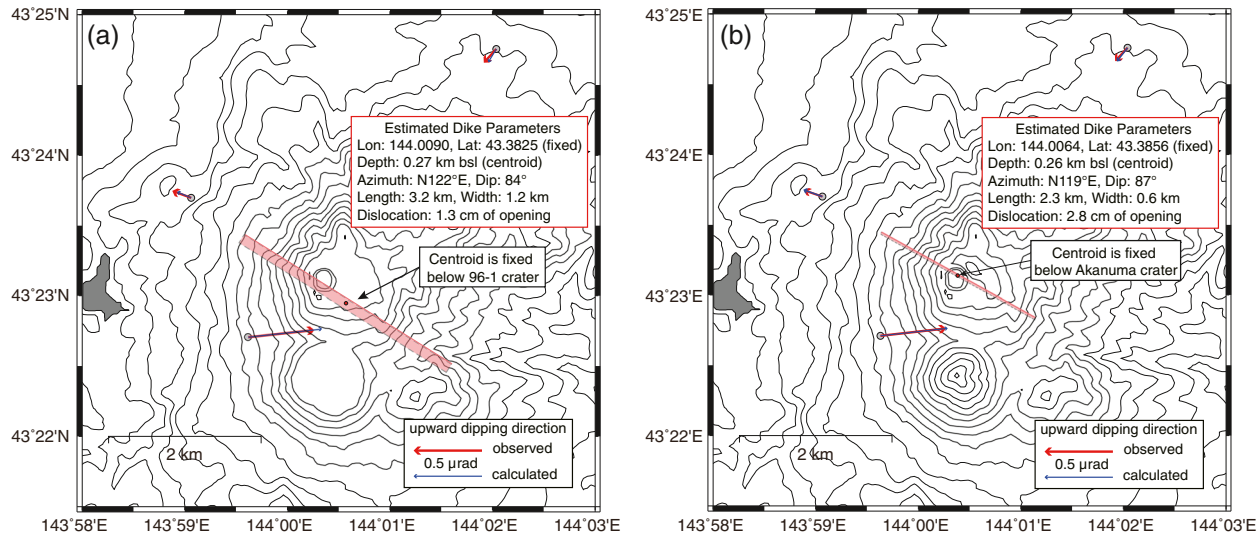

Fig. 6 Best-fit solutions of rectangle dike model. **a** The centroid of the dike is fixed below the 96-1 crater, where the 2008 eruption occurred. **b** The centroid of the dike is fixed below the Akanuma crater, which is the central crater of the Pon-Machineshiri crater area. *Red thick* and *blue thin arrows* express observed and calculated tilt vectors, respectively. The *orange-colored side of the rectangle* indicates the upper edge of the dike

and Oshima 2008). This deflation was considered as a result of phase change of the volcanic fluid and fluid migration at the source area.

The 2008 event was successfully observed at three stations. Moreover, we confirmed that an inflation of the dike oriented in the NW–SE direction below the Pon-Machineshiri crater effectively explains the observed tilt vectors in this study. The fact that the tilt vectors at MEA in 2006 and 2008 showed almost the same direction suggests the possibility that the dike estimated from the 2008 activity can also explain the tilt vector observed in 2006. Unfortunately, however, we were unable to determine which source configuration, dike or sphere, is better for the 2006 data because of the limited number of recorded data. It is expected that future activity at Meakan-dake volcano will provide an opportunity for obtaining a more concrete understanding of the precursory deformation source below the Pon-Machineshiri crater.

In addition to the summit active craters of Pon-Machineshiri and Naka-Machineshiri, several fuming grounds and flowing hot springs are distributed around the volcano. Figure 7 shows a map view of these features in which a few linear distributions of craters, fuming grounds, and hot springs crossing the volcanic edifice are evident. Yuno-taki hot spring, one of the tourist spots near Meakan-dake, is located about 3 km SW of Pon-Machineshiri. In the opposite direction of the volcano, fuming grounds are present on the NE slope about 2 km northeast of Naka-Machineshiri. More specifically, Yuno-taki, Pon-Machineshiri, Naka-Machineshiri, and the NE fuming grounds are aligned in the NE–SW direction. The other two alignments are in the NW–SE direction, one of which passes through the Pon-Machineshiri crater. In the summit area of Pon-Machineshiri, the 2006 Akanuma and 96-1 craters almost align in the NW–SE direction. Meakan Onsen hot spring is located on the extended line of this alignment. A hot spring at the eastern foot of the volcano can be regarded as belonging to a NW–SE orientation passing through Naka-Machineshiri. These alignments generally resemble conjugate structures and may reflect a hydrothermal system beneath the volcano. In Fig. 7, we also show a horizontal projection of the estimated dike (case 1). The dike direction is highly consistent with the alignment of craters and hot springs passing through Pon-Machineshiri in the NW–SE direction. This fact also suggests the existence of hydrothermal structures at this location.

Ogiso and Yomogita (2012) attempted to estimate the source location of the precursory tremors of the 2008 activity by using the spatial distribution of seismic amplitudes recorded at short-period seismic stations of JMA Sapporo. They used the method developed by Battaglia and Aki (2003) and Kumagai et al. (2010) to analyze three tremors occurring on September 29, November 16, and November 17–19. According to their results, despite the site amplification correction using coda waves of local earthquakes, the estimated locations of the tremor sources were shifted southward about 1 km from the summit rather than appearing just below the Pon-Machineshiri crater (e.g., Figure 15 in Ogiso and Yomogita 2012). They examined the shift by using the dataset of volcano tectonic (VT) earthquakes that are routinely analyzed by manual

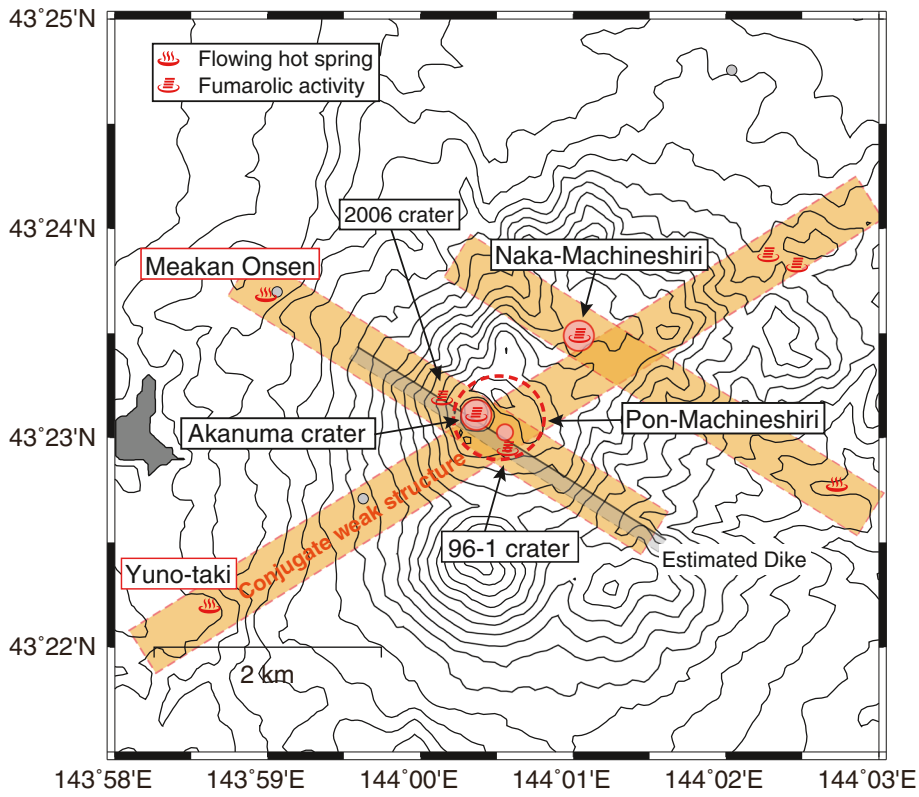

Fig. 7 Distribution of major fumarolic areas and hot springs around Meakan-dake volcano. Strong fuming activities are evident at the Pon-Machineshiri crater and at Naka-Machineshiri. An additional fuming ground is located at about 2 km northeast of the summit area. Flowing hot springs are distributed at the foot of the volcano. Major hot springs Meakan Onsen and Yuno-taki are located at the western side. An additional hot spring flows from the opposite side of the volcano. *Orange-colored hatches* correspond to the alignment of surface hydrothermal activities. The orientation of the estimated dike model in Fig. 6a is also shown

selection of P and S arrivals and confirmed that a similar location shift appeared when they applied the same analysis to VT earthquakes estimated below the Pon-Machineshiri crater (Figure 8 in Ogiso and Yomogita 2012). In light of this location shift, the source location of the volcanic tremor on November 16 shown in Figure 15 in Ogiso and Yomogita (2012) can be regarded as close to the Pon-Machineshiri crater, which is the assumed location of the centroid of the dike in this study.

According to temporal changes in seismic amplitude ratio among JMA stations, Ogiso and Yomogita (2012) divided the November 16 tremor into three phases. Phase 1 includes the first 4 min from the beginning of the tremor (0:57–1:01 JST). During this phase, the amplitude of the tremor gradually increases. Phase 2 includes the next 4 min during the amplitude decreasing stage (1:01–1:05 JST), and phase 3 includes the later part (after 1:05 JST). The tilt change in this study began around 0:59 JST and continued for about 3 min, corresponding to the transition between phases 1 and 2. During this transition, Ogiso and Yomogita (2012) estimated a change in source depth to the deeper part. However, we were unable to find an evident phase to reflect the transition in the tilt records.

Almost at the same time as the occurrence of the November 16 volcanic tremor, very local surface deformation was observed around the Pon-Machineshiri crater, as was an increase in groundwater level at Akanko Onsen (Ishimaru et al. 2009). The local deformation around the crater was detected by GNSS receivers installed at the north and south sides of the crater, identified respectively as NSY and PMN (Fig. 8). The horizontal distance between these two receivers is about 1.0 km. The southern receiver at PMN moved about 4 mm westward and about 1 mm northward relative to the northern receiver at NSY. The observed motion is represented by a blue arrow in Fig. 8. Based on the dike opening model in this study, we estimated the theoretical relative motion between these GNSS stations. The red arrow in Fig. 8 shows the expected motion from our model (case 1). The vector directions were quite consistent, although the scale of the red arrow in the figure is smaller than that of the blue arrow by 1 order of magnitude. To explain this motion more effectively than the single dike theory estimated here, the opening displacement of the dike must have been larger by 1 order of magnitude. However, such a large aperture is

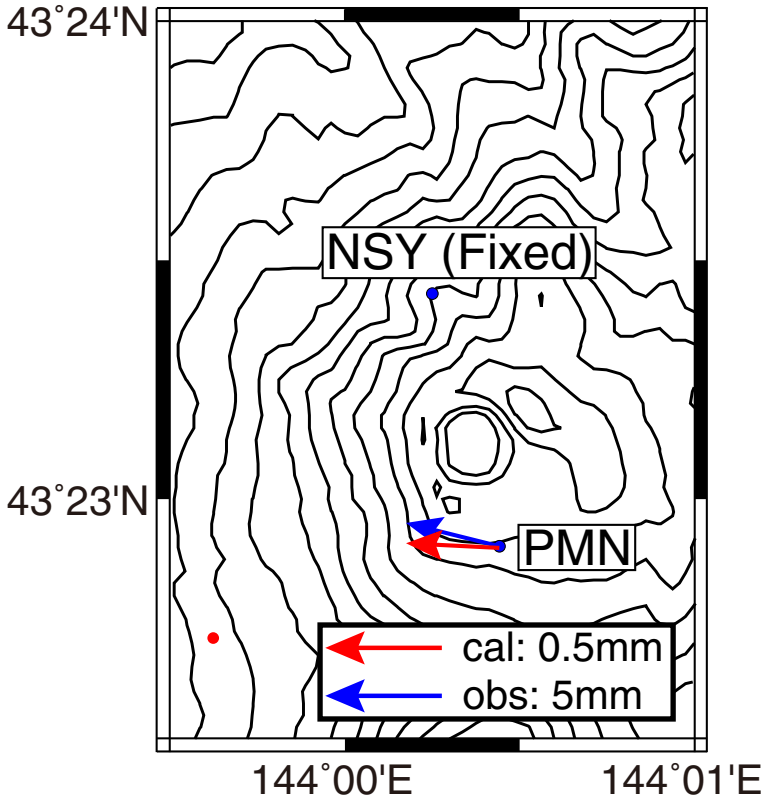

Fig. 8 Relative motions of GNSS stations close to the Pon-Machineshiri crater. The *blue arrow* expresses the horizontal movement of PMN relative to NSY reported in Ishimaru et al. (2009). The *red arrow* is the expected relative displacement from the dike model shown in Fig. 6a. The baseline distance between the GNSS stations is about 1 km

inconsistent with our tilt data observed at the three stations. For this deformation, Ishimaru et al. (2009) reported that the relative motion between GNSS stations occurred at around 2:00 JST on November 16. If the time of deformation given by Ishimaru et al. (2009) is exact, a 1-h delay of ground deformation is present from the volcanic tremor that we analyzed. To check their description, we carefully examined seismic and geodetic data from our monitoring stations, although but no notable signal was identified at around 2:00 JST. Additionally, the sampling interval of the graph of temporal variation in the GNSS baseline shown by Ishimaru et al. (2009) appeared to be one dataset per hour. Therefore, we conclude that the temporal inconsistency between the tremor and the GNSS data arose from the low temporal resolution of GNSS data. The difference in magnitude of the motion vector may have been caused by a topographic effect or an uncertainty of a heterogeneous underground structure that was not evaluated in our forward calculation.

A step change in groundwater level was observed at AK1 well at Akanko Onsen during 1:00–1:30 JST on November 16, which is almost the same time as that of the volcanic tremor (Ishimaru et al. 2009). Long duration of the water level change in the well can be attributed to the dispersion property of underground water in the permeable layer around the well. Recently, a proportionality factor between the changes in water level at this well and in ambient volumetric strain was estimated on the basis of the M2 tidal constituent as 3.42 mm/10^{-8} strain (Takahashi et al. 2012). By using this factor, the observed increase in water level of about 3 cm at the AK1 well was transferred to changes in volumetric strain of about 88 nstrain of compression. Based on our dike model (case 1), the expected change in volumetric strain at Akanko Onsen, about 8 km NE of Meakan-dake volcano, is 18 nstrain of compression. Although this value is about one fifth of the observed value, the theoretical change in strain is fairly consistent with the observed water level change at AK1 despite the uncertainty of the heterogeneous underground structure. These results also support our simple dike model.

The ground deformation analyzed in this study is considered to be one of the preparatory processes of phreatic activities because the opening of the dike occurred at a shallow depth only 2 days prior to the first eruption. At Meakan-dake volcano, the preparatory processes usually began a few months before the eruption, which

appeared as an increase in seismicity observed in 1988, 1996, 2006, and 2008. From the recent phreatic eruptions in 2006 and 2008, in addition to an increase in seismicity, it is confirmed that small ground deformation preceded the eruptions. Although increases in seismicity without following surface activities were sometimes observed at Meakan-dake, we have not observed detectable ground deformation during such isolated periods of seismic unrest. Ground deformation coinciding with an increase in seismicity can be considered as an indication of progress in the preparation processes toward phreatic eruptions; therefore, we can conclude that such activity is an important precursory signal of phreatic eruption, especially in Meakan-dake. The results of this study provide the following conceivable theory of volcanic activity. For the 2008 eruption, preparatory accumulation of thermal energy began in late September during the first seismic swarm. When sufficient energy was accumulated at a certain depth, the precursory dike opening was induced beneath the Pon-Machineshiri crater at around 1:00 JST on November 16. Two days later, a small phreatic eruption occurred at the 96-1 crater on the SE perimeter of the Pon-Machineshiri crater.

Conclusions

We successfully observed precursory volcano deformation of small phreatic eruptions at Meakan-dake volcano in November 2008. The deformation occurred along with a small volcanic tremor, which is the same as that occurring in February 2006. The observed tilt changes at three stations were effectively explained by an almost vertical opening dike beneath the summit of the Pon-Machineshiri crater with a volume increase of $4–5 \times 10^4$ m^3. The NW–SE strike of this is highly consistent with the alignment of active craters and hot springs on and around the volcano. This coincidence strongly suggests that hydrothermally weak structures beneath the volcano were activated prior to the eruption. The model estimated in this study should be re-examined at the next occurrence of such activity.

Tilt changes detected at Meakan-dake were quite small, on the order of 1 μrad or less. This may be a lower limit in magnitude for extracting significant signals from the original data, particularly for surface stations constructed in convenient locations. However, if adequate monitoring systems are developed around the volcano, it is expected that we can observe small deformation indicating unrest of underground hydrothermal systems prior to phreatic eruptions. We strongly expect that similar precursory ground deformation will be found at other active volcanoes. Increasing the number of examples of precursory phenomena will help to reduce the risk of disaster from phreatic eruptions.

Competing interests

The authors declare that they have no competing interests.

Authors' contributions

Both authors have spent time and effort to maintain continuous operation of the monitoring stations used in this study. Both authors have read and approved the final manuscript.

Acknowledgements

We appreciate all staff members at the Volcano Observation and Information Center, Sapporo District Meteorological Observatory, Japan Meteorological Agency, who provided us with a list of volcanic earthquakes of Meakan-dake. We also thank Dr. Takeshi Hashimoto, Dr. Hitoshi Mori, Mr. Tokumitsu Maekawa, and Mr. Atsuo Suzuki at ISV, Hokkaido University, who spent a considerable amount of time assisting with our volcano observation. Moreover, we acknowledge Dr. Hiroaki Takahashi for providing detailed information about groundwater monitoring at Akanko Onsen. We also thank two anonymous reviewers for quick and constructive responses that improved the manuscript. Some figures were prepared by using Generic Mapping Tools software (Wessel and Smith 1991).

Author details

[1]Institute of Seismology and Volcanology, Faculty of Science, Hokkaido University, N10W8, Kita-ku, Sapporo, Hokkaido 060-0810, Japan. [2]Usu Volcano Observatory, Institute of Seismology and Volcanology, Faculty of Science, Hokkaido University, Tatsuka 142, Sobetsu, Hokkaido 052-0106, Japan.

Received: 19 January 2015 Accepted: 4 July 2015
Published online: 29 July 2015

References

Aoyama H (2008) Simplified test on tilt response of CMG40T seismometers (in Japanese with English abstract). Bull Volcanol Soc Jpn 53:35–46

Aoyama H, Oshima H (2008) Tilt change recorded by broadband seismometer prior to small phreatic explosion of Meakan-dake volcano, Hokkaido, Japan. Geophys Res Lett 35, L06307. doi:10.1029/2007GL032988

Barberi F, Bertagnini A, Landi P, Principe C (1992) A review on phreatic eruptions and their precursors. J Volcanol Geotherm Res 52:231–246

Battaglia J, Aki K (2003) Location of seismic events and eruptive fissures on the Piton de la Fournaise volcano using seismic amplitudes. J Geophys Res 108:2364. doi:10.1029/2002JB002193

Feuillard M, Allegre CJ, Brandeis G, Gaulon R, Mouel JLLE, Mercier JC, Pozzi JP, Semet MP (1983) The 1975–1977 crisis of la Soufriere de Guadeloupe (F.W.I): a still-born magmatic eruption. J Volcanol Geotherm Res 16:317–334

Genco R, Ripepe M (2010) Inflation-deflation cycles revealed by tilt and seismic records at Stromboli volcano. Geophys Res Lett 37, L12302. doi:10.1029/2010GL042925

Germanovich LN, Lowell RP (1995) The mechanism of phreatic eruptions. J Geophys Res 100(5):8417–8434

Graizer V (2006) Tilts in strong ground motion. Bull Seismol Soc Am 96:2090–2102

Hirose W, Okazaki N, Ishimaru S, Hasegawa K, Fujiwara S, Nakagawa M, Sasaki H, Satou J, Observatory SDM, Observatory KLM (2007a) The eruption on March 2006 at Meakandake volcano, Hokkaido, Japan: eruption process and ash fall survey (in Japanese with English abstract). Rep Geol Surv Hokkaido 78:37–55

Hirose W, Nakagawa M, Takarada S, Yoshida M, Okazaki N, Ishimaru S, Sasaki H, Arai K, Kodama Y, Satou J, Observatory SDM, Observatory KLM (2007b) November 1996 & November 1998 eruptions at Meakandake volcano, eastern Hokkaido, Japan (in Japanese with English abstract). Rep Geol Surv Hokkaido 78:21–35

Ishimaru S, Tamura M, Hirose W, Murayama Y, Okazaki N, Shibata T, Nakagawa M, Yoshimoto M, Hasegawa K, Uesawa S, Nishimoto J, Kosugi A, Matsumoto A, Baba A, Sasaki H, Takahashi H, Ichiyanagi M, Yamaguchi T, Kohno Y, Honda R, Kasahara M, Observatory SDM, Observatory KLM, Observatory ALM (2009) Preliminary report on the eruption on November 2008 of Meakandake volcano (in Japanese with English captions). Rep Geol Surv Hokkaido 80:115–126

Japan Meteorological Agency (2013) National catalogue of the active volcanoes in Japan (the fourth edition). http://www.data.jma.go.jp/svd/vois/data/tokyo/STOCK/souran_eng/menu.htm. Accessed 7 Jan 2015

Kasahara M (1988) On small eruptions of Meakandake volcano in the eastern part of Hokkaido, Japan (January-February, 1988) (in Japanese with English captions). Bull Volcanol Soc Jpn 33(4):379–381
Kumagai H, Nakano M, Maeda T, Yepes H, Palacios P, Ruiz M, Arrais S, Vaca M, Molina I, Yamashina T (2010) Broadband seismic monitoring of active volcanoes using deterministic and stochastic approaches. J Geophys Res 115, B08303. doi:10.1029/2009JB006889
Lisowski M (2007) Analytical volcano deformation source models. In: Dzurisin D (ed) Volcano deformation, geodetic monitoring techniques. Springer-Praxis, Chichester
Mastin LG (1991) The roles of magma and groundwater in the phreatic eruptions at Inyo Craters, Long Valley Caldera, California. Bull Volcanol 53:579–596
Matsumoto S, Shimizu H, Matsushima T, Uehira K, Yamashita Y, Nakamoto M, Miyazaki M, Chikura H (2013) Short-term spatial change in a volcanic tremor source during the 2011 Kirishima eruption. Earth Planets Space 65:323–329. doi:10.5047/eps.2012.09.002
Murase T (1957) Geophysical studies of volcanoes in Hokkaido, Japan. Part 6. On the small earthquakes originated under the volcano Me'akan-dake (in Japanese with English abstract). Geophys Bull Hokkaido Univ 5:5–9
Murase T, Onda I, Seino M, Nogoshi M (1960) Geophysical studies of volcanoes in Hokkaido, Japan. Part 8. Activity of volcano Me'akan-dake in 1959 (in Japanese with English abstract). Geophys Bull Hokkaido Univ 7:93–103
Nakamichi H, Yamanaka Y, Terakawa T, Horikawa S, Okuda T, Yamazaki F (2013) Continuous long-term array analysis of seismic records observed during the 2011 Shinmoedake eruption activity of Kirishima volcano, southwest Japan. Earth Planets Space 65:551–562. doi:10.5047/eps.2013.03.002
Ogiso M, Yomogita K (2012) Migration of tremor locations before the 2008 eruption of Meakandake volcano, Hokkaido, Japan. J Volcanol Geotherm Res 217-218:8–20. doi:10.1016/j.jvolgeores.2011.12.005
Okada Y (1992) Internal deformation due to shear and tensile faults in a half-space. Bull Seismol Soc Am 82:1018–1040
Sakuma S, Murase T (1957) Recent activity of volcano Me'akan-dake. J Fac Sci Hokkaido Univ (Ser 7) 1:21–36
Takahashi H, Shibata T, Yamaguchi T, Ikeda R, Okazaki N, Akita F (2012) Volcanic strain change prior to an earthquake swarm observed by groundwater level sensors in Meakan-dake, Hokkaido, Japan. J Volcanol Geotherm Res 215–216:1–7. doi:10.1016/j.jvolgeores.2011.11.006
Takeo M, Maehara Y, Ichihara M, Ohminato T, Kamata R, Oikawa J (2013) Ground deformation cycles in a magma-effusive stage, and sub-Plinian and Vulcanian eruptions at Kirishima volcanoes, Japan. J Geophys Res 118:4758–4773. doi:10.1002/jgrb.50278
Wada K (1991) Mixing and evolution of magmas at Me-Akan volcano, Eastern Hokkaido, Japan. Bull Volcanol Soc Jpn 36(1):61–78
Wada K (1998) Meakandake (in Japanese). In: Takahashi M, Kobayashi T (eds) Field guide of volcano in Japan 3. Volcanoes in Hokkaido. Tsukijishokan, Tokyo, pp 20–40
Wessel P, Smith WHF (1991) Free software helps map and display data. EOS Trans 296 AGU 72:445–446
Williams CA, Wadge G (1998) The effect of topography on magma chamber deformation models: application to Mt. Etna and radar interferometry. Geophys Res Lett 25:1549–1552
Yokoyama I, Katsui Y, Ehara S, Koide K (1976) Meakandake. Volcano geology, eruption history, current activities and disaster prevention measures (in Japanese). Hokkaido Disaster Management Council, Sapporo

Submit your manuscript to a SpringerOpen journal and benefit from:

- ► Convenient online submission
- ► Rigorous peer review
- ► Immediate publication on acceptance
- ► Open access: articles freely available online
- ► High visibility within the field
- ► Retaining the copyright to your article

Submit your next manuscript at ► springeropen.com